Volume 1
Number 4
August 2025
Pages 433-660

EES Solar

rsc.li/EESSolar

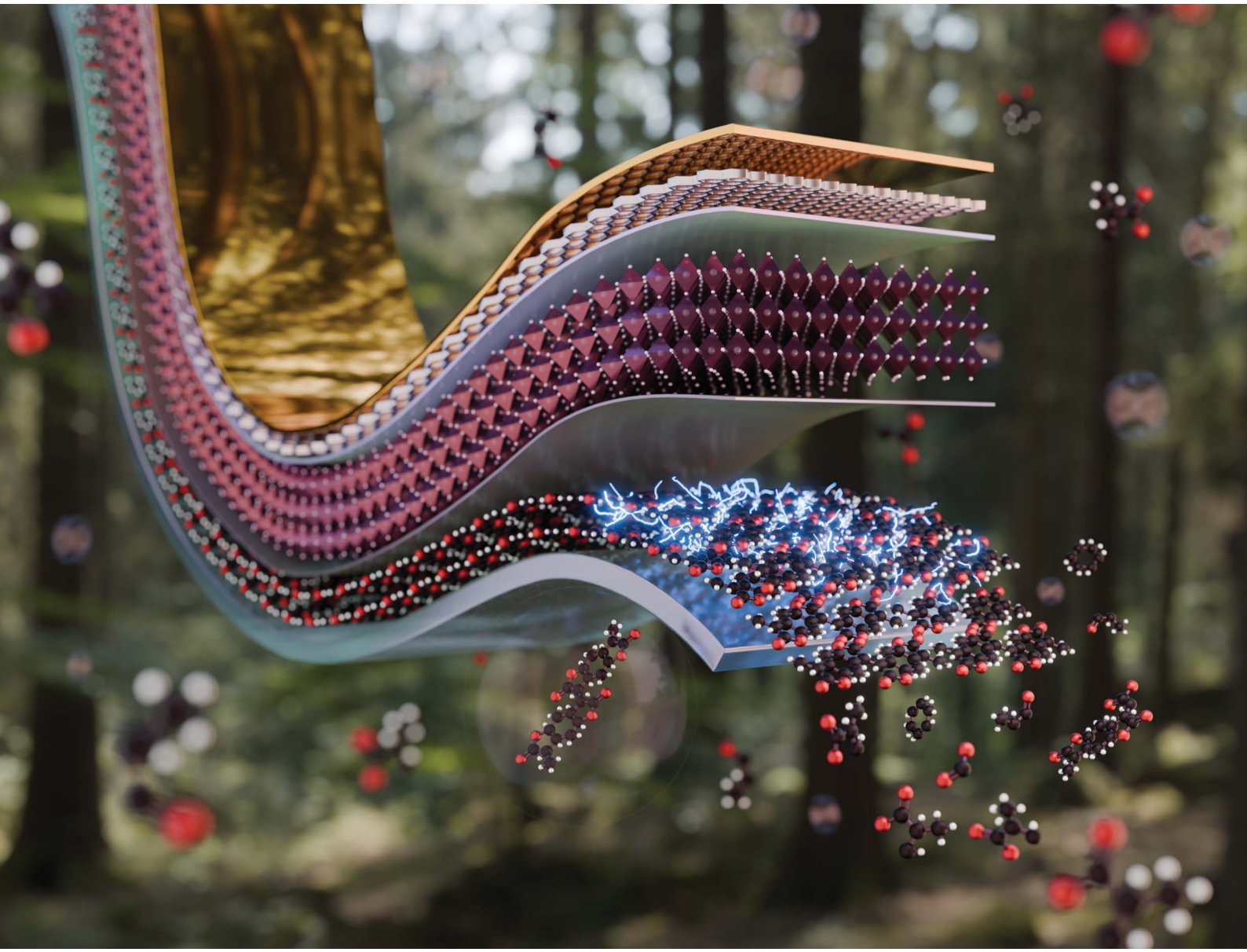

ISSN 3033-4063

ROYAL SOCIETY OF CHEMISTRY

PAPER

Jianguo Mei, Letian Dou *et al.*
Enabling ITO-free perovskite solar cells through n-doped poly(benzodifurandione) (n-PBDF) electrodes

EES Solar

PAPER

View Article Online
View Journal | View Issue

Cite this: *EES Sol.*, 2025, **1**, 529

Enabling ITO-free perovskite solar cells through n-doped poly(benzodifurandione) (n-PBDF) electrodes†

Prashant Kumar, ‡[ab] Won-June Lee, ‡[c] Yuanhao Tang, ‡[a] Hanjun Yang, [ac] Wenzhan Xu, [a] Priyanka Rout, [c] Liyan You,[c] Joseph A. Romo, [c] Basudev Pradhan, [b] Jianguo Mei *[c] and Letian Dou *[acd]

The burgeoning commercialization of perovskite solar cells (PSCs) is propelled by their exceptional power conversion efficiency (PCE), enhanced stability, and ease of fabrication. However, the rigidity of mainstream transparent conductive oxides (TCOs) limits the adaptability of PSCs to various application scenarios. Although alternative materials such as silver nanowires, carbon nanotubes, graphene, and PEDOT:PSS have been evaluated, the p-type nature confines their device designs to inverted architecture and restricts broader applicability. Here, for the first time, a conducting polymer electrode based on n-doped poly(benzodifurandione) (n-PBDF) was used to replace TCOs in PSCs. The n-PBDF electrodes can be readily fabricated *via* low-temperature, solution-based processes, indicating substantial potential for reducing manufacturing costs. Furthermore, its integration into PSCs has negligible effect on the phase, morphology, or photophysical properties of the perovskite layer, which is comparable to the typical TCOs. After optimization, the n-PBDF-based device achieves a power conversion efficiency of 12.70 and 11.23%, for rigid and flexible devices, respectively. Our study provides a promising alternative to the widely used TCOs in PSCs, highlighting the advantages of using n-doped conducting polymers in terms of processability and flexibility.

Received 20th March 2025
Accepted 26th May 2025

DOI: 10.1039/d5el00035a

rsc.li/EESSolar

Broader context

The rising demand for solar energy has fueled significant advancements in perovskite photovoltaic technology, emphasizing the need for materials that balance high performance and cost efficiency. A major contributor to solar cell costs is the use of transparent conductive oxides (TCOs), particularly indium tin oxide (ITO). In response, n-doped poly(benzodifurandione) (n-PBDF), a cutting-edge n-type conductive transparent polymer, has emerged as a noteworthy alternative. When utilized as the front electrode, n-PBDF offers numerous advantages, including cost-effectiveness, ease of solution-based processing, enhanced flexibility, reduced brittleness, and scalability for industrial production. These attributes lower manufacturing costs while improving the durability and adaptability of photovoltaic devices. Moreover, n-PBDF can be applied to large areas using roll-to-roll coating or screen printing, potentially replacing traditional transparent conductive electrodes and boosting the economic feasibility of perovskite solar cells. Solar cells incorporating n-PBDF as the front electrode have demonstrated remarkable power conversion efficiencies (PCEs) of 12.70% for rigid devices and 11.23% for flexible devices. This demonstrates n-PBDF's potential to drive the next generation of high-performance, cost-effective, and scalable solar technologies, enabling wider adoption in commercial solar applications.

Introduction

The dawn in the commercialization of perovskite solar cells (PSCs) has paced up significantly in recent years,[1–3] driven primarily by their impressive power conversion efficiency (PCE), improved operational stability, and simpler and cost-effective fabrication processes.[4,5] Among the various components of PSCs, transparent conductive oxide (TCO) electrodes, predominantly indium tin oxide (ITO) and fluorine-doped tin oxide (FTO), account for approximately 56% of the overall cost of solar modules and contribute significantly to the environmental impact.[6–8] Moreover, their inherent brittleness significantly limits their utility in flexible and wearable photovoltaic technologies, necessitating the development of alternative materials to meet the demands of emerging flexible applications.

Alternative transparent electrodes, including silver nanowires (AgNWs),[9] carbon nanotubes (CNTs),[10] graphene,[11] and conducting polymers such as poly(3,4-ethylenedioxythiophene):poly(4-

[a]*Davidson School of Chemical Engineering, Purdue University, West Lafayette, IN 47907, USA. E-mail: dou10@purdue.edu*

[b]*Department of Energy Engineering, Central University of Jharkhand, Ranchi, 835222, India*

[c]*James Tarpo Jr. and Margaret Tarpo Department of Chemistry, Purdue University, West Lafayette, IN 47907, USA. E-mail: jgmei@purdue.edu*

[d]*Birck Nanotechnology Center, Purdue University, West Lafayette, IN 47907, USA*

† Electronic supplementary information (ESI) available. See DOI: https://doi.org/10.1039/d5el00035a

‡ These authors contributed equally to this work.

styrenesulfonate) (PEDOT:PSS),[12,13] have been extensively investigated to replace traditional TCOs. In particular, PEDOT:PSS has drawn significant interest due to its solution processability, flexibility, and compatibility with large-area printing techniques crucial for commercialization. Early attempts using low-temperature processed PEDOT:PSS as an alternative to ITO resulted in PSCs achieving efficiencies of around 10.5%.[14] Recently, Zhang *et al.* replaced ITO electrodes in PSCs with single-walled carbon nanotubes, achieving improved chemical stability, lower manufacturing costs, and a PCE of 19% on rigid substrates and 18% for flexible devices.[10] However, PEDOT:PSS and carbon nanotubes are intrinsically p-type, restricting their use mainly to inverted (p–i–n) device structures. Furthermore, PEDOT:PSS typically suffers from limited electron transport capability, instability under certain operational conditions, and difficulty in maintaining optimal performance with thicker films required for scalable printing processes.[15,16] Consequently, there is an urgent demand for novel n-type conductive polymers that not only overcome these intrinsic limitations of PEDOT:PSS but also reach TCO benchmarks.

Recently, n-doped poly(benzodifurandione) (n-PBDF) has emerged as a promising candidate.[17] Unlike rigid and expensive ITO substrates, n-PBDF electrodes offer the advantages of low-cost, low-energy, solution-based processing methods and greater flexibility, thus significantly reducing production costs and environmental impact.[17–20] Specifically, n-PBDF offers high conductivity, a low work function (~4.6 eV), and inherent solution processability, making it well-suited for PSC applications.

In this study, we propose employing n-PBDF as an alternative front electrode material in ITO-free PSCs. Notably, when employing n-PBDF electrodes, key properties of the perovskite layer, such as the crystal phase, morphology, surface roughness, and photoluminescence characteristics, remain comparable to those observed with conventional ITO electrodes, demonstrating excellent compatibility. After optimization, PSCs with n-PBDF electrodes without any different surface/additional layers achieved a promising PCE of 12.70% with a comparable open-circuit voltage (V_{oc}) of 1.06 V. These results highlight the significant potential of n-PBDF as an effective, flexible, and sustainable alternative for PSC applications independent of conventional TCO materials.

Results and discussion

The n-type conducting polymer, n-PBDF, offers significant advantages due to its compatibility with solution-processing techniques, such as spin-coating,[17,19,20] inkjet printing,[21] and blade coating[22] enabling its application on both rigid glass and flexible polyethylene terephthalate (PET) substrates. In this study, spray-coating[18] was employed to fabricate n-PBDF films, resulting in a uniform deposition on both glass and PET substrates (Fig. 1a, b, and S1†). This solution-based approach leverages the inherent advantages of solution processing, including low-cost fabrication due to minimal material waste and the flexibility to tailor film properties, such as thickness and morphology, through straightforward adjustments in processing parameters. The uniform drying of the wet film, formed by the deposited polymer solution on the substrates, plays a key role in producing high-quality n-PBDF films with consistent conductivity without additional complex procedures.

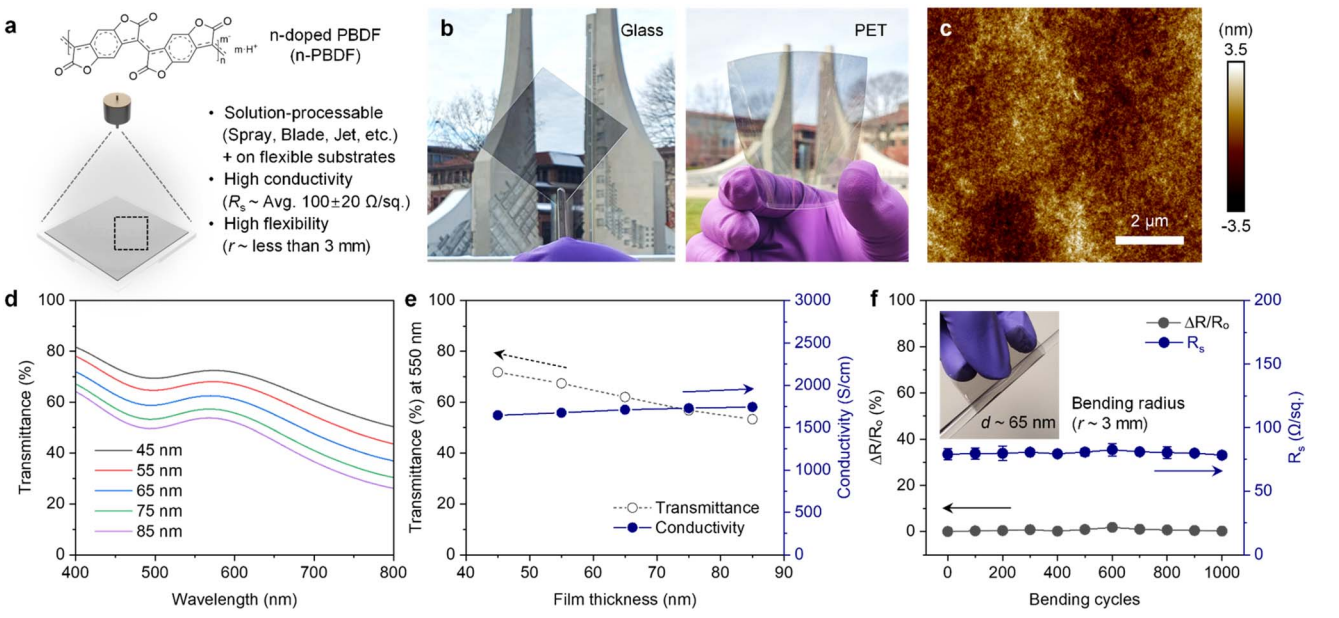

Fig. 1 (a) Schematic overview of the preparation of n-type conducting polymer (n-PBDF) film. (b) Photographs of the n-PBDF films coated on a rigid glass substrate and a flexible PET substrate. (c) AFM height image of n-PBDF films. (d) Transmittance spectra of n-PBDF films with varying thicknesses in the visible light range (baseline: glass substrate in ambient air). (e) Variations in specific transmittance at 550 nm derived from (d) and electrical conductivity calculated from sheet resistance as a function of the n-PBDF film thickness. (f) Sheet resistance changes of the n-PBDF flexible electrode after a bending test (1000 cycles, bending radius < 3 mm).

Moreover, the fabrication of n-PBDF films was conducted under ambient conditions and did not require high-temperature annealing or additional solvent post-treatment. This makes it particularly suitable for thermally sensitive flexible substrates and highlights a clear differentiation from other conductive polymers, such as PEDOT:PSS, which typically necessitate subsequent thermal annealing and solvent treatments (*e.g.*, ethylene glycol, acidic solvents) to enhance crystallinity and film conductivity.[15,23] Additionally, n-PBDF maintains its intrinsically high conductivity without the need for additives such as inorganic nanocomposites (*e.g.*, AgNWs, CNTs, *etc.*), thereby simplifying the fabrication process and improving stability, distinguishing it from other organic conducting materials. The film uniformity was evaluated using optical microscopy at the macroscale, which shows a homogeneous coating without notable defects across the substrate (Fig. S2†). Surface roughness, analyzed *via* atomic force microscopy (AFM, Fig. 1c), revealed a root mean square surface roughness (R_q) of approximately 2.31 nm, demonstrating a smooth and uniform surface at the nanoscale. An important step in replacing the ITO layer with an n-PBDF electrode is verifying that its work function (WF) closely matches that of ITO and aligns effectively with the energy level of the adjacent layer. We measured the WF of n-PBDF films using Kelvin probe force microscopy, obtaining a value of 4.64 eV, comparable to the widely used 4.7 eV of ITO for photovoltaic applications (Fig. S3†).

The transmittance of the n-PBDF substrates exhibited high transparency across the visible spectrum, confirming their potential as front electrodes in perovskite solar cells (Fig. 1d). As thickness increases, transmittance decreases while sheet resistance also decreases (*e.g.*, 139.8–67.0 Ω sq^{-1} over thicknesses of 45–85 nm, for scalable spray-coated films). Although these sheet resistance values are higher than those of conventional ITO substrates (<10–20 Ω sq^{-1} at 120–300 nm, sputtered films), the selected thickness range of 65–75 nm (90.9–78.8 Ω sq^{-1}) provides a suitable balance between transparency and conductivity (Fig. 1e). Additionally, long-term stability tests showed that the electrical properties of n-PBDF films remained stable after more than three months of storage in the solar cell fabrication environment, demonstrating their practical suitability for practical applications (Fig. S4†). Unlike ITO,[24] which is prone to cracking or interfacial delamination under mechanical stress, leading to reduced optical and electrical performance, n-PBDF-coated flexible substrates exhibit superior durability. Bending tests at a 3 mm radius over 1000 cycles only resulted in negligible changes in the sheet resistance, highlighting the suitability of the materials for flexible device applications (Fig. 1f).

To further investigate the suitability of the n-PBDF film on perovskite crystallization, scanning electron microscopy (SEM) was conducted to gain insight into the surface morphology of the samples (Fig. 2a and b). The SEM images show that the perovskite grown on n-PBDF has a grain size comparable to that

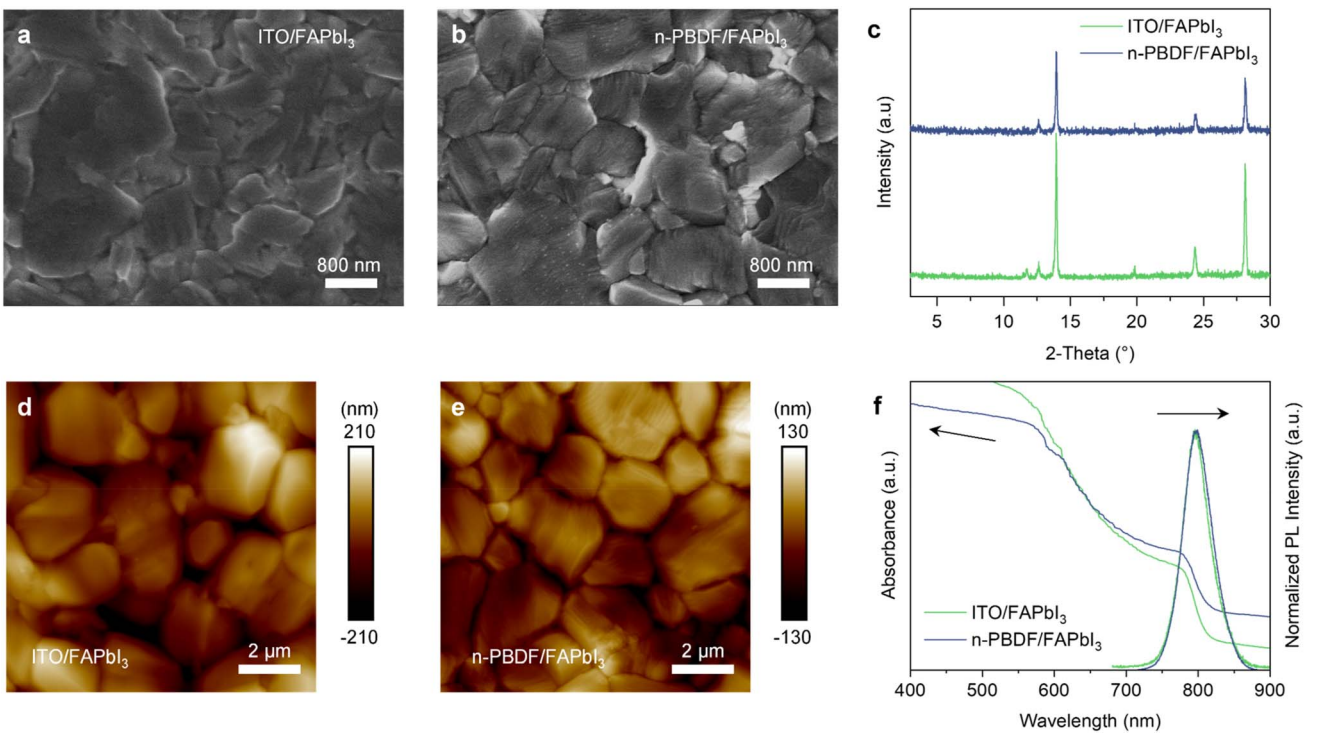

Fig. 2 SEM images of perovskite ($FAPbI_3$) grown on (a) ITO and (b) n-PBDF electrodes on the glass substrate. (c) XRD spectra of perovskite grown on the ITO and n-PBDF electrodes. AFM height images of perovskite grown on the (d) ITO and (e) n-PBDF electrodes. (f) UV-vis and PL spectra of perovskite grown on ITO and n-PBDF electrodes.

on ITO, indicating that substituting n-PBDF for ITO does not alter perovskite morphology. X-ray diffraction (XRD) further confirmed that the replacement of ITO with n-PBDF does not affect the phase of $FAPbI_3$ perovskite (Fig. 2c). Notably, whereas the control exhibits some δ-phase at around 12°, the perovskite grown on n-PBDF displays no δ-phase, reflecting better crystallization.

AFM measurements were then performed to assess the R_q of the perovskite layers grown on n-PBDF (Fig. 2d and e). Interestingly, the R_q for the perovskite grown on n-PBDF (40.6 nm) is even lower than that grown on the ITO (66.9 nm), indicating a smoother surface. As shown in ultraviolet-visible and photoluminescence (PL) spectra (Fig. 2f), the perovskite grown on ITO and n-PBDF exhibits the same exciton feature and similar absorption characteristics, while the n-PBDF-based film shows a higher overall absorbance due to the absorption of n-PBDF itself. Then, time-resolved PL was performed to explore the carrier dynamics. SnO_2 as an electron transport layer (ETL) was also coated on both ITO and n-PBDF for comparison. The results show that the perovskites grown on n-PBDF and on ITO exhibit similar lifetimes at short time scales for electron extraction, suggesting that substituting n-PBDF for ITO does not compromise the charge extraction capability of SnO_2 (Fig. S5†). Interestingly, it can be observed that the perovskite on n-PBDF/SnO_2 exhibits a longer carrier lifetime (approximately 164.07 ns) than that on ITO (107.89 ns). This prolonged carrier lifetime on n-PBDF may be attributed to larger perovskite crystal grains and potentially fewer defects, likely due to the smooth and intrinsically ordered structures[25,26] of n-PBDF reducing nucleation sites and promoting uniform crystallization.

The n–i–p device was fabricated by following the procedure described in the experimental section in the ESI.†[27] The fabricated device stack and corresponding cross-section SEM clearly demonstrate the architecture of the PSC (Fig. 3a–c). The energy level diagram and the work function (WF) of the n-PBDF electrode are well-matched with the energy level of SnO_2, which enhances the efficient transport of electrons to the front electrode (Fig. 3d). To examine the photovoltaic performance, the current–voltage (J–V) characteristics were recorded under

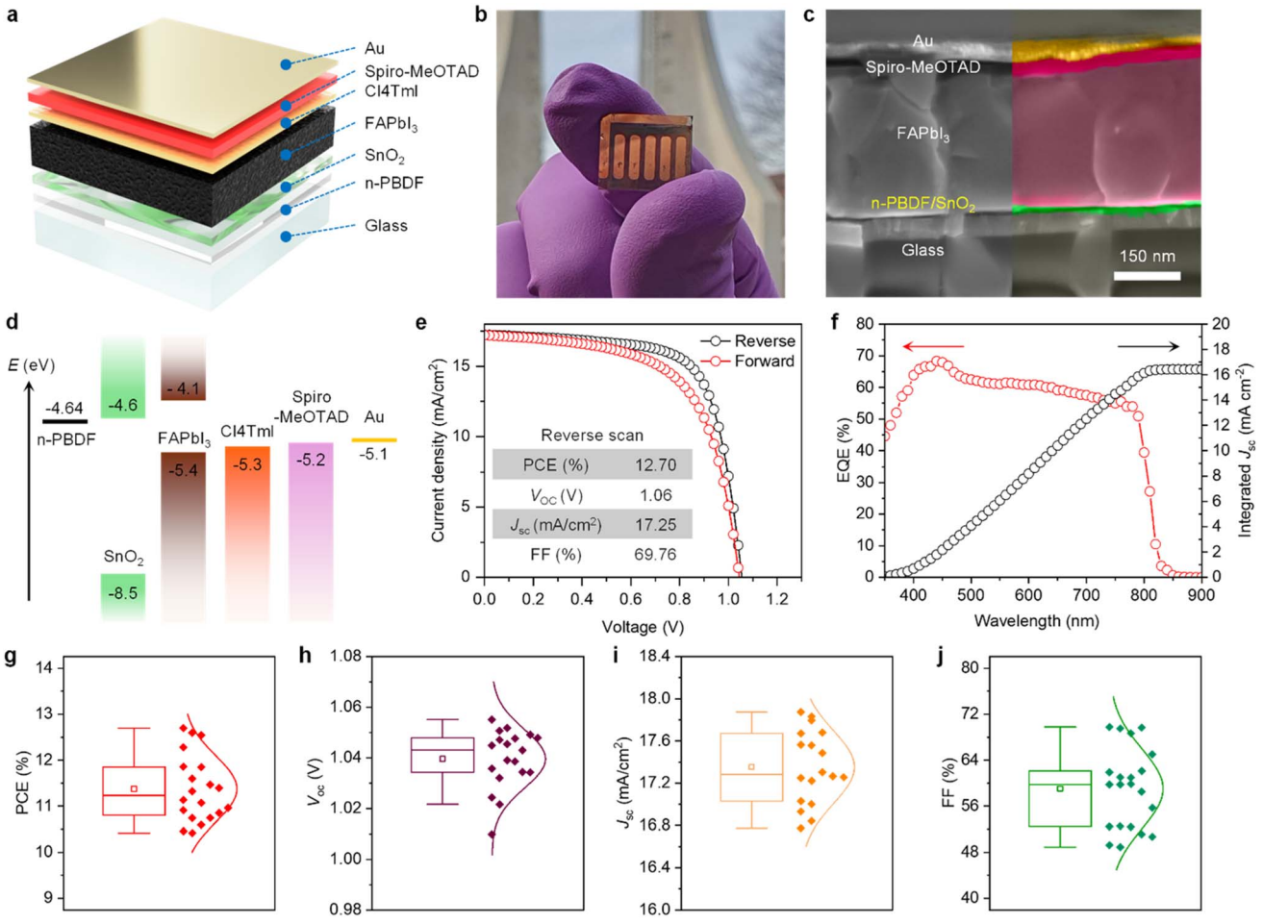

Fig. 3 (a) Schematic and (b) photograph of the rigid n-PBDF-based PSC device. (c) Cross-sectional SEM image of the device with the structure of glass/n-PBDF/SnO_2/perovskite ($FAPbI_3$)/Cl4TmI/spiro-MeOTAD/Au. (d) Energy band alignment of the component layers in the n-PBDF-based PSC. (e) J–V characteristics and (f) EQE with corresponding integrated J_{sc}. (g–j) Statistical results of the rigid n-PBDF-based PSC devices (from three batches, $n = 20$).

standard testing conditions (Fig. 3e). The optimized n-PBDF-based device achieved the highest power conversion efficiency (PCE) of 12.70%, with an open-circuit voltage (V_{oc}) of 1.055 V, a short-circuit current density (J_{sc}) of 17.25 mA cm^{-2}, and a fill factor (FF) of 69.76%. These results represent the first reported performance of such a configuration, showcasing promising efficiency levels. The J_{sc} value was further validated by external quantum efficiency (EQE) measurements, which indicated a calculated integrated J_{sc} of 16.4 mA cm^{-2}. Statistical analysis of the photovoltaic parameters (Fig. 3g–j) demonstrated excellent reproducibility of both J_{sc} and V_{oc}, at approximately 17 mA cm^{-2} and 1.04 V, respectively. It is noted that due to the relatively low J_{sc} and FF, the performance of n-PBDF-based devices is lower compared to typical devices (Fig. S6a†), which could be further improved in the future.

Light soaking tests without encapsulation showed a performance decrease in n-PBDF-based perovskite solar cells after 50 hours of continuous illumination, indicating a need for potential improvement in long-term stability (Fig. S7†). This decrease may result from moisture-induced charge traps in the perovskite layer, chemical instability at the interface between SnO_2 and n-PBDF film, or residual moisture and oxygen trapped in the n-PBDF film during fabrication.[28] As a soft polymer material, n-PBDF may permit relatively larger moisture and oxygen permeability than the solid-state sputtered ITO, indicating a need for proper device encapsulation. Additionally, photo-generated oxidative species could lower the doping level of n-PBDF film, contributing to perovskite defects, but its moisture affinity and potential redoping effects[26] suggest possibilities for improving stability. These findings suggest scope for improving n-PBDF film stability through encapsulation and material optimization to enhance long-term device stability.

The applicability of n-PBDF in flexible solar cells was also evaluated using flexible PET substrates (Fig. 4a and b). After optimization, the flexible n-PBDF-based device yielded a PCE of 11.24%, a V_{oc} of 1.04 V, a J_{sc} of 18.289 mA cm^{-2}, and an FF of 54.67% (Fig. 4c). For comparison, the J–V characteristics of control substrates were also recorded, yielding a PCE of 18.91%, with a V_{oc} of 1.12 V, J_{sc} of 24.22 mA cm^{-2}, and a FF of 69.4% (Fig. S6c†). The statistical results show the potential of n-PBDF for application in flexible photovoltaics, although the FF value

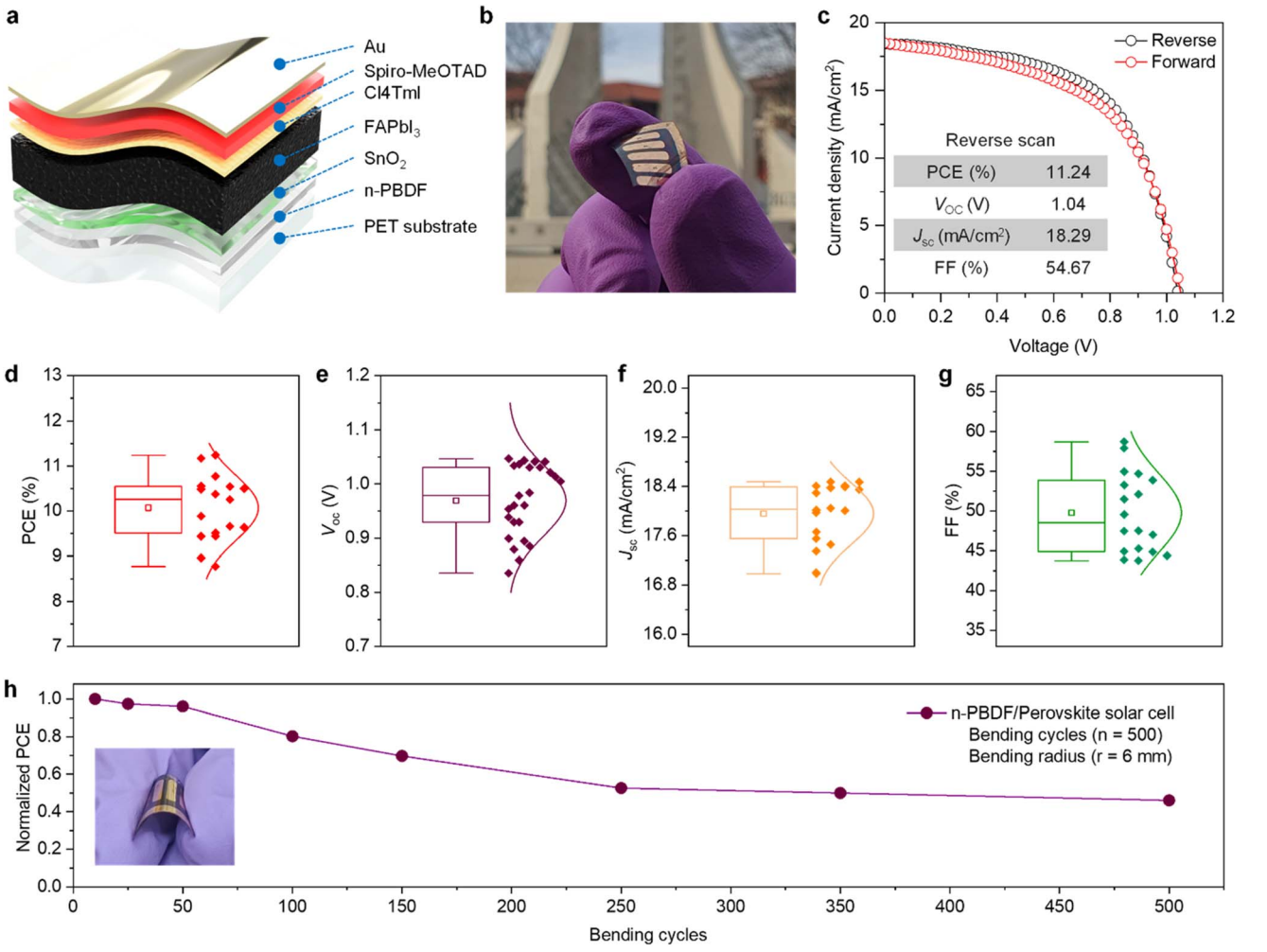

Fig. 4 (a) Schematic and (b) photograph of the flexible n-PBDF-based PSC device. (c) J–V characteristics and (d–g) statistical results of the flexible n-PBDF-based PSC devices (from three batches, n > 18). (h) Bending cycle stability test of the flexible n-PBDF-based PSC device.

is lower compared to typical rigid devices, suggesting that further optimization in this area may be necessary to improve overall device performance (Fig. 4d–g). Moreover, the device performances are highly reproducible, with minimal variation.

To assess the mechanical durability of the n-PBDF-based flexible device, a bending test was conducted with a bending radius of 6 mm, simulating the stress that flexible devices might encounter in practical applications. After 100 bending cycles, the device retained 80% of its initial efficiency, demonstrating a commendable level of mechanical stability (Fig. 4h). These results suggest that the n-PBDF-based flexible device exhibits promising durability under mechanical stress, which is critical for real-world applications such as wearable electronics or curved photovoltaics where bending is frequent.

While n-PBDF-based perovskite solar cells demonstrate promising performance, their efficiency and stability can be further improved to compete with ITO-based devices. Techniques such as interface passivation, precise perovskite layer tuning, and n-PBDF/ETL interface engineering with refined coatings or buffer layers may enhance charge extraction and stability. Additionally, minimizing dedoping and improving optical transparency of the conducting polymer could boost further performance, offering potential for cost-effective and high performance flexible perovskite solar cells.

Conclusions

To summarize, we have successfully developed an ITO-free device by replacing the conventional transparent conductive oxides with the n-PBDF polymer layer. This innovative approach achieved a power conversion efficiency of 12.70% for rigid substrates and 11.24% for flexible substrates, demonstrating the potential of n-PBDF for both types of substrates. Remarkably, the device was able to retain 50% of its initial efficiency after 500 bending cycles, showcasing moderate mechanical durability. Furthermore, to the best of our knowledge, this is the first reported use of an n-type polymer as a transparent conducting polymer in perovskite solar cells, marking a significant step toward the development of sustainable and flexible photovoltaic technologies. With its high conductivity, transparency, and flexibility, n-PBDF shows potential for advancing flexible perovskite solar cells and related optoelectronic applications beyond conventional TCOs.

Data availability

The data that support the findings of this study are available from the corresponding author upon reasonable request.

Author contributions

J. M. and L. D. conceived the idea and supervised the project. P. K., W.-J. L., and Y. T. fabricated the samples, validated the results, visualized the data, and wrote the first draft of the work. W.-J. L. conducted the synthesis, scalable fabrication, and characterization with the help of L. Y. J. R. and P. R. helped with thermal/optical analyses and KPFM measurements, respectively. H. Y. and W. X. assisted with the XRD and TRPL measurements and device fabrication. R. P. provided support with data validation. J. M. and L. D. guided the project discussions, reviewing, and editing. All the authors contributed to the discussion of the results and the final manuscript preparation.

Conflicts of interest

J. M. is a cofounder of Ambilight, which sponsors this study under a research agreement. He is also a founder of PBDF LLC, focusing on the commercialization of n-PBDF. All other authors declare no conflict of interest.

Acknowledgements

This work is primarily supported by the U.S. Department of Energy's Office of Energy Efficiency and Renewable Energy (EERE) under the Solar Energy Technologies Office Award DE-EE0009519 and DE-EE 0011513. W.-J. L., P. R., L. Y., and J. M. acknowledge the support from Ambilight Inc. under contract #4000187.02. P. K. would like to acknowledge the Overseas Visiting Doctoral Fellowship, Anusandhan National Research Foundation (ANRF), Government of India. J. R. acknowledges the support from the Center for Soft PhotoElectroChemical Systems, an Energy Frontier Research funded by Department of Energy, Office of Science, Basic Energy Sciences, under award #DE-SC0023411.

References

1 X. Tian, S. D. Stranks, J. Huang, V. M. Fthenakis, Y. Yang and F. You, *Energy Environ. Sci.*, 2025, **18**, 194–213.
2 A. K. Jena, A. Kulkarni and T. Miyasaka, *Chem. Rev.*, 2019, **119**, 3036–3103.
3 M. V. Khenkin, E. A. Katz, A. Abate, G. Bardizza, J. J. Berry, C. Brabec, F. Brunetti, V. Bulović, Q. Burlingame, A. Di Carlo, R. Cheacharoen, Y.-B. Cheng, A. Colsmann, S. Cros, K. Domanski, M. Dusza, C. J. Fell, S. R. Forrest, Y. Galagan, D. Di Girolamo, M. Grätzel, A. Hagfeldt, E. von Hauff, H. Hoppe, J. Kettle, H. Köbler, M. S. Leite, S. Frank Liu, Y.-L. Loo, J. M. Luther, C.-Q. Ma, M. Madsen, M. Manceau, M. Matheron, M. McGehee, R. Meitzner, M. K. Nazeeruddin, A. F. Nogueira, Ç. Odabaşı, A. Osherov, N.-G. Park, M. O. Reese, F. De Rossi, M. Saliba, U. S. Schubert, H. J. Snaith, S. D. Stranks, W. Tress, P. A. Troshin, V. Turkovic, S. Veenstra, I. Visoly-Fisher, A. Walsh, T. Watson, H. Xie, R. Yıldırım, S. M. Zakeeruddin, K. Zhu and M. Lira-Cantu, *Nat. Energy*, 2020, **5**, 35–49.
4 P. Kumar, A. Mahapatra and B. Pradhan, in *Perovskite Optoelectronic Devices*, ed. B. Pradhan, Springer International Publishing, Cham, 2024, pp. 149–214.
5 X. Liu, D. Luo, Z.-H. Lu, J. S. Yun, M. Saliba, S. I. Seok and W. Zhang, *Nat. Rev. Chem.*, 2023, **7**, 462–479.
6 V. Larini, C. Ding, F. Faini, G. Pica, G. Bruni, L. Pancini, S. Cavalli, M. Manzi, M. Degani, R. Pallotta, M. De

Bastiani, C.-Q. Ma and G. Grancini, *Adv. Funct. Mater.*, 2024, **34**, 2306040.
7 Z. Song, C. L. McElvany, A. B. Phillips, I. Celik, P. W. Krantz, S. C. Watthage, G. K. Liyanage, D. Apul and M. J. Heben, *Energy Environ. Sci.*, 2017, **10**, 1297–1305.
8 J. Lim, N.-G. Park, S. I. Seok and M. Saliba, *Energy Environ. Sci.*, 2024, **17**, 4390–4425.
9 B.-T. Liu, Y.-Y. Zuo, C.-H. Wang, T.-F. Hong and Y.-F. Chen, *ACS Appl. Nano Mater.*, 2023, **6**, 19108–19115.
10 J. Zhang, X. Hu, H. Li, K. Ji, B. Li, X. Liu, Y. Xiang, P. Hou, C. Liu, Z. Wu, Y. Shen, S. D. Stranks, S. R. P. Silva, H.-M. Cheng and W. Zhang, *Adv. Funct. Mater.*, 2021, **31**, 2104396.
11 J. O'Sullivan, M. Wright, X. Niu, P. Miller, P. R. Wilshaw and R. S. Bonilla, *Prog. Photovolt. Res. Appl.*, 2023, **31**, 1478–1492.
12 B. Vaagensmith, K. M. Reza, M. N. Hasan, H. Elbohy, N. Adhikari, A. Dubey, N. Kantack, E. Gaml and Q. Qiao, *ACS Appl. Mater. Interfaces*, 2017, **9**, 35861–35870.
13 K. Sun, P. Li, Y. Xia, J. Chang and J. Ouyang, *ACS Appl. Mater. Interfaces*, 2015, **7**, 15314–15320.
14 T. Liu, L. Zuo, T. Ye, J. Wu, G. Xue, W. Fu and H. Chen, *RSC Adv.*, 2015, **5**, 94752–94758.
15 X. Fan, W. Nie, H. Tsai, N. Wang, H. Huang, Y. Cheng, R. Wen, L. Ma, F. Yan and Y. Xia, *Adv. Sci.*, 2019, **6**, 1900813.
16 B. J. Worfolk, S. C. Andrews, S. Park, J. Reinspach, N. Liu, M. F. Toney, S. C. B. Mannsfeld and Z. Bao, *Proc. Natl. Acad. Sci. U. S. A.*, 2015, **112**, 14138–14143.
17 Z. Ke, A. Abtahi, J. Hwang, K. Chen, J. Chaudhary, I. Song, K. Perera, L. You, K. N. Baustert, K. R. Graham and J. Mei, *J. Am. Chem. Soc.*, 2023, **145**, 3706–3715.
18 G. Liu, H.-H. Hsu, S. Samal, W.-J. Lee, Z. Ke, L. You, B. M. Savoie and J. Mei, *Angew. Chem., Int. Ed.*, 2025, **64**, e202418668.
19 I. Song, W.-J. Lee, Z. Ke, L. You, K. Chen, S. Naskar, P. Mehra and J. Mei, *Nat. Electron.*, 2024, **7**, 1158–1169.
20 J. H. Kim, I. Lee, W.-J. Lee, D. Shin, H. Lee, L. Q. Flagg, J. Chaudhary, L. You, K. Kang, J. Mei and S. Park, *Mater. Sci. Eng., R*, 2025, **165**, 101003.
21 I. Brunetti, N. James Pataki, D. R. Hinojosa, A. Hawkey, O. Karakaya, C. Rainer, M. I. Khan, L. Franke, M. M. Mallick, G. Hernandez-Sosa, M. Kemerink, M. Caironi and U. Lemmer, *Adv. Mater. Technol.*, 2025, **10**, 2400968.
22 H. Tang, Z. Xu, Y. Liang, W. Cui, Y. Chen, Q. Jiang, T. Lei, Y. Ma and F. Huang, *Angew. Chem., Int. Ed.*, 2025, **64**, e202415349.
23 Y. Xu, Z. Lin, W. Wei, Y. Hao, S. Liu, J. Ouyang and J. Chang, *Nano-Micro Lett.*, 2022, **14**, 117.
24 C. Peng, Z. Jia, H. Neilson, T. Li and J. Lou, *Adv. Eng. Mater.*, 2013, **15**, 250–256.
25 H. Tang, Y. Liang, C. Liu, Z. Hu, Y. Deng, H. Guo, Z. Yu, A. Song, H. Zhao, D. Zhao, Y. Zhang, X. Guo, J. Pei, Y. Ma, Y. Cao and F. Huang, *Nature*, 2022, **611**, 271–277.
26 Z. Ke, J. Chaudhary, L. Q. Flagg, K. N. Baustert, A. O. Yusuf, G. Liu, L. You, K. R. Graham, D. M. DeLongchamp and J. Mei, *Adv. Funct. Mater.*, 2024, **34**, 2400255.
27 K. Ma, J. Sun, H. R. Atapattu, B. W. Larson, H. Yang, D. Sun, K. Chen, K. Wang, Y. Lee, Y. Tang, A. Bhoopalam, L. Huang, K. R. Graham, J. Mei and L. Dou, *Sci. Adv.*, 2023, **9**, eadg0032.
28 N. Ahn, K. Kwak, M. S. Jang, H. Yoon, B. Y. Lee, J.-K. Lee, P. V. Pikhitsa, J. Byun and M. Choi, *Nat. Commun.*, 2016, **7**, 13422.